Available online at http://scik.org
J. Math. Comput. Sci. 7 (2017), No. 3, 468-484
ISSN: 1927-5307

A MULTI-REGIONS SEIS DISCRETE EPIDEMIC MODEL WITH A TRAVEL-BLOCKING VICINITY OPTIMAL CONTROL APPROACH ON CELLS

KANZA CHOUAYAKH[1], MOSTAFA RACHIK[2], OMAR ZAKARY[2] AND ILIAS ELMOUKI[2,*]

[1]Laboratory of Computer Science, Imaging and Digital Analysis, Department of Mathematics and Computer Sciences, Faculty of Sciences Dhar El Mahraz, Sidi Mohamed Ben Abdellah University of Fez, Morocco

[2]Laboratory of Analysis, Modeling and Simulation, Department of Mathematics and Computer Science, Hassan II University of Casablanca. BP 7955, Sidi Othman, Casablanca, Morocco

Abstract. In Susceptible-Exposed-Infected-Susceptible (SEIS) compartmental models, an infected population is divided into two categories; symptomatic infected individuals represented by the I variable, and asymptomatic infected individuals, people who are not yet infectious, or those who are just exposed to infection, represented by the variable E. In these models, an infected population recovers with no immunity, and then, it moves immediately to the susceptible compartment once it becomes recovered, For this, we devise a multi-regions SEIS discrete-time model which describes infection dynamics when an epidemic is emerging in regions that are connected with their neighbors by movement. The main goal from this kind of modeling, is to introduce after, controls variables which restrict movements of the infected individuals coming from the vicinity of the region targeted by our control strategy, called here; the travel-blocking vicinity optimal control approach. A grid of colored cells is presented to illustrate the whole domain affected by the epidemic while each cell represents a sub-domain or region. The infection is supposed starting from only one cell located in one of the corners of the grid, while the region aiming to control, is supposed to be located in the 4th line and 7th column of the grid, as an example to show the effectiveness of the proposed control strategy when it is applied to a cell with 8 neighboring cells.

Keywords: multi-regions model; SEIS epidemic model; discrete-time model; optimal control; vicinity; travel-blocking.

2010 AMS Subject Classification: 93C15, 34B15.

*Corresponding author
E-mail address: i.elmouki@gmail.com
Received January 20, 2017; Published May 1, 2017

1. Introduction

Susceptible-Exposed-Infected-Susceptible (SEIS) epidemic models have been applied to situations in which some individuals are infected by some typical epidemics which do not necessarily imply the appearance of symptoms, and where it is considered that an infected population moves immediately to the susceptible compartment after being recovered from an infection due to the lack of immunization. This kind of compartmental models is very useful to model the evolution of many phenomena in different situations, see as examples, subjects treated in [1],[2].

In 2016, Zakary et al. published their papers in [3],[4],[5] and [6], where they have presented a new modeling approach based on multi-regions discrete-time SIR models, with applications to HIV/AIDS and Ebola diseases in the continuous-time case. All their models have aimed to describe the spatial-temporal evolution of epidemics which emerge in different geographical regions and to show the influence of one region on an other region via infection travel. The authors have also devised other multi-regions compartmental models in the discrete-time case, for the study of infection spatial-temporal spread using SIRS and SEIRS systems [7],[8] and which involve discrete cellular simulations. Here, we are more interested to devise a mathematical model, which is based on multi-regions SEIS discrete-time interactions, for describing the spatial spread of an epidemic that emerges in a global domain of interest Ω represented by a grid of colored cells, uniform in size. These cells are connected by movements of their populations, and they represent sub-domains of Ω or regions, noting that only one of these cells, that is targeted by our control strategy.

Zakary et al. represented in [3], each region by a sub-domain $(\Omega_j)_{j=1,..,p}$ while here, each region or cell is denoted by $(C_{pq})_{p,q=1,..,M}$.

For this, we assume that the epidemic can be transmitted and propagated by movements of people, from one spatial cell C_{pq}, to its neighbors or cells belonging to its vicinity. In fact, depending on different geographical scales, a cell C_{pq} can either represent a farm, city or country, etc. This means these present cellular representations, can be useful for the study of infection

dynamics regardless of the area size, and also, regions are not necessarily attached but it is sufficient to suppose any kind of connection between them. Furthermore, we choose an optimization criteria which is based on the travel-blocking optimal control strategy as in [7],[8] and which aims to restrict movements of people coming from one or more cells and intending to enter other cells. Then, we seek to minimize an objective function associated to C_{pq} and which is subject to its associated discrete-time system with control functions introduced to show the effectiveness of the travel-blocking operations when they are followed between C_{pq} and its neighbors. We denote by V_{pq}, the vicinity set, and which is composed by all neighboring cells of C_{pq}, denoted by $(C_{rs})_{r=p+k,s=q+k'}$ with $(k,k') \in \{-1,0,1\}^2$ except when $k = k' = 0$. As we have mentioned before, these cells are observed they are attached in the grid, however, in reality, they are not necessarily joined together. With the consideration of the travel-blocking vicinity optimal control approach, we can then show, the impact of the optimal blocker controls on reducing contacts between susceptible people of the targeted cell C_{pq} and infected people coming from one cell C_{rs} or more cells from V_{pq}.

The paper is organized as follows: Section 2. presents the discrete-time multi-cells SEIS epidemic system based on a cellular modeling approach. In Section 3., we announce a theorem of necessary conditions and characterization of the sought optimal controls functions. Finally, in section 4., we provide simulations of the numerical results for an example of 100 cells when an infection starts from one cell of them and which has 3 neighboring cells, while aiming to control only one cell with 8 neighboring cells.

2. **The mathematical SEIS model**

In this section, we consider a multi-regions discrete-time epidemic model which describes the spatial-temporal and regional spread of an epidemic based on SEIS interactions within a global domain of interest Ω, divided to M^2 regions or cells, uniform in size. This domain can be represented by the union $\Omega = \bigcup_{p,q=1}^{M} C_{pq}$ with $(C_{pq})_{p,q=1,\dots,M}$; a spatial location or region.

The S-E-I-S dynamics associated to a cell C_{pq} are noted by the states $S_i^{C_{pq}}, E_i^{C_{pq}}$ and $I_i^{C_{pq}}$, and we

note that the transition between them, is probabilistic, with probabilities being determined by the observed characteristics of specific diseases. In addition to the death, there are population movements among these three epidemiological compartments, from time unit i to time $i+1$. We assume the susceptible individuals are those who are not yet infected but can be infected only through contacts with $I_i^{C_{pq}}$ coming from V_{pq} (Vicinity set or Neighborhood of a cell C_{pq}), thus, the infection transmission is assumed to occur between individuals that are present in a given cell C_{pq}, and it is given by

$$\sum_{C_{rs}\in V_{pq}} \beta_{rs} I_i^{C_{rs}} S_i^{C_{pq}}$$

where β_{rs} is the constant proportion of adequate contacts between a susceptible from a cell C_{pq} and an infective coming from its neighbor cell $C_{rs} \in V_{pq}$ with

V_{pq}=$\left\{ C_{rs} \in \Omega / r = p+k, s = q+k', (k,k') \in \{-1,0,1\}^2 \right\} \setminus C_{pq}$.

The SEIS dynamics associated to domain or cell C_{pq}, are described based on the following multi-regions discrete-time model

For $p,q = 1,\ldots,M$, we have

$$\begin{aligned} S_{i+1}^{C_{pq}} &= S_i^{C_{pq}} - \beta_{pq} I_i^{C_{pq}} S_i^{C_{pq}} - \sum_{C_{rs}\in V_{pq}} \beta_{rs} I_i^{C_{rs}} S_i^{C_{pq}} \\ &\quad - d S_i^{C_{pq}} + \theta I_i^{C_{pq}} \end{aligned} \tag{2.1}$$

$$E_{i+1}^{C_{pq}} = E_i^{C_{pq}} + \beta_{pq} I_i^{C_{pq}} S_i^{C_{pq}} + \sum_{C_{rs}\in V_{pq}} \beta_{rs} I_i^{C_{rs}} S_i^{C_{pq}} - (\gamma + d) E_i^{C_{pq}} \tag{2.2}$$

$$I_{i+1}^{C_{pq}} = I_i^{C_{pq}} + \gamma E_i^{C_{pq}} - (\alpha + d + \theta) I_i^{C_{pq}} \tag{2.3}$$

$i = 0,\ldots,N-1$

with $S_0^{C_{pq}} \geqslant 0$, $E_0^{C_{pq}} \geqslant 0$ and $I_0^{C_{pq}} \geqslant 0$ are the given initial conditions.

$d > 0$ is the natural death rate while $\alpha > 0$ is the death rate due to the infection and $\theta > 0$ denotes the recovery rate. By assuming that all regions are occupied by homogeneous populations, α, d and θ are considered to be the same for all cells of Ω. γ is defined as the average incubation period.

3. The travel-blocking vicinity optimal control approach

The main goal of the travel-blocking vicinity optimal control approach is to restrict movements of infected people coming from the set V_{pq} and aiming to reach the cell C_{pq}. For this, we introduce controls variables $u^{pqC_{rs}}$ which limit contacts between susceptibles of the targeted cell C_{pq} and infectives from cells C_{rs} that belong to V_{pq}. Then, for a given cell C_{pq} in Ω, the discrete-time system (2.1)-(2.3) becomes

$$\begin{aligned} S_{i+1}^{C_{pq}} &= S_i^{C_{pq}} - \beta_{pq} I_i^{C_{pq}} S_i^{C_{pq}} - \sum_{C_{rs} \in V_{pq}} u_i^{pqC_{rs}} \beta_{rs} I_i^{C_{rs}} S_i^{C_{pq}} \\ &\quad - d S_i^{C_{pq}} + \theta I_i^{C_{pq}} \end{aligned} \tag{3.1}$$

$$E_{i+1}^{C_{pq}} = E_i^{C_{pq}} + \beta_{pq} I_i^{C_{pq}} S_i^{C_{pq}} + \sum_{C_{rs} \in V_{pq}} u_i^{pqC_{rs}} \beta_{rs} I_i^{C_{rs}} S_i^{C_{pq}} - (\gamma + d) E_i^{C_{pq}} \tag{3.2}$$

$$I_{i+1}^{C_{pq}} = I_i^{C_{pq}} + \gamma E_i^{C_{pq}} - (\alpha + d + \theta) I_i^{C_{pq}} \tag{3.3}$$

$i = 0, \ldots, N-1$

Our goal concerns the minimization of the number of the infected people and the cost of the travel-blocking vicinity optimal control approach. For this, we consider an optimization criterion associated to cell C_{pq}, defined by the following objective function

$$\begin{aligned} J_{pq}(u^{pqC_{rs}}) &= A_1 I_N^{C_{pq}} \\ &\quad + \sum_{i=0}^{N-1} \left(A_1 I_i^{C_{pq}} + \sum_{C_{rs} \in V_{pq}} \frac{A_{rs}}{2} (u_i^{pqC_{rs}})^2 \right) \end{aligned} \tag{3.4}$$

where $A_1 > 0$ and $A_{rs} > 0$ are the constant severity weights associated to the number of infected individuals and controls respectively. The controls functions are defined in the control set U_{pq} associated to the cell C_{pq}, represented by the set

$$\begin{aligned} U_{pq} &= \{u^{pqC_{rs}} \, measurable / u^{min} \leq u_i^{pqC_{rs}} \leq u^{max}, \; u^{max} < 1 \; u^{min} > 0, \\ &\quad i = 0, \ldots, N-1, C_{rs} \in V_{pq}\} \end{aligned} \tag{3.5}$$

Then, we seek optimal controls $u^{pqC_{rs}*}$ such that

$$J_{pq}(u^{pqC_{rs}*}) = min\{J_{pq}(u^{pqC_{rs}})/u^{pqC_{rs}} \in U_{pq}\}$$

The sufficient conditions for the existence of optimal controls in the case of discrete-time epidemic models have been announced in [3],[4],[17] and [18].

As regards to the necessary conditions and the characterization of the discrete optimal controls, we use a discrete version of Pontryagin's maximum principle [3],[4],[19].

For this, we define an Hamiltonian $\mathscr{H}$ associated to a cell C_{pq} by

$$\begin{aligned}
\mathscr{H} &= A_1 I_i^{C_{pq}} + \sum_{C_{rs}\in V_{pq}} \frac{A_{rs}}{2}(u_i^{pqC_{rs}})^2 \\
&+ \zeta_{1,i+1}^{C_{pq}} \Big[S_i^{C_{pq}} - \beta_{pq} I_i^{C_{pq}} S_i^{C_{pq}} \\
&\quad - \sum_{C_{rs}\in V_{pq}} u_i^{pqC_{rs}} \beta_{rs} I_i^{C_{rs}} S_i^{C_{pq}} - d S_i^{C_{pq}} + \theta I_i^{C_{pq}} \Big] \\
&+ \zeta_{2,i+1}^{C_{pq}} \left[E_i^{C_{pq}} + \beta_{pq} I_i^{C_{pq}} S_i^{C_{pq}} + \sum_{C_{rs}\in V_{pq}} u_i^{pqC_{rs}} \beta_{rs} I_i^{C_{rs}} S_i^{C_{pq}} - (\gamma + d) E_i^{C_{pq}} \right] \\
&+ \zeta_{3,i+1}^{C_{pq}} \Big[I_i^{C_{pq}} + \gamma E_i^{C_{pq}} - (\alpha + d + \theta) I_i^{C_{pq}} \Big]
\end{aligned}$$

$i = 0, ..., N-1$

with $\zeta_{k,i}^{C_{pq}}$, $k = 1,2,3$, the adjoint variables associated to $S_i^{C_{pq}}, E_i^{C_{pq}}$ and $I_i^{C_{pq}}$ respectively, and defined based on formulations of the following theorem.

Theorem 3.1. *(Necessary Conditions & Characterization)*

Given optimal controls $u^{pqC_{rs}*}$ *and solutions* $S_i^{C_{pq}^*}, E_i^{C_{pq}^*}$ *and* $I_i^{C_{pq}^*}$*, there exists* $\zeta_{k,i}^{C_{pq}}, i = 0...N, k = 1,2,3$*, the adjoint variables satisfying the following equations*

$$\triangle\zeta_{1,i}^{C_{pq}} = -\left[(1-d)\,\zeta_{1,i+1}^{C_{pq}} + \left(\beta_{pq} I_i^{C_{pq}} + \sum_{C_{rs}\in V_{pq}} u_i^{C_{rs}} \beta_{rs} I_i^{C_{rs}}\right)\left(\zeta_{2,i+1}^{C_{pq}} - \zeta_{1,i+1}^{C_{pq}}\right)\right] \tag{3.6}$$

$$\triangle\zeta_{2,i}^{C_{pq}} = -\left[\gamma\left(\zeta_{3,i+1}^{C_{pq}} - \zeta_{2,i+1}^{C_{pq}}\right) + (1-d)\,\zeta_{2,i+1}^{C_{pq}}\right] \tag{3.7}$$

$$\triangle\zeta_{3,i}^{C_{pq}} = -\left[A_1 + \beta_{pq} S_i^{C_{pq}}\left(\zeta_{2,i+1}^{C_{pq}} - \zeta_{1,i+1}^{C_{pq}}\right) + \theta\left(\zeta_{1,i+1}^{C_{pq}} - \zeta_{3,i+1}^{C_{pq}}\right) + (1-\alpha-d)\,\zeta_{3,i+1}^{C_{pq}}\right] \tag{3.8}$$

with $\zeta_{1,N}^{C_{pq}} = 0, \zeta_{2,N}^{C_{pq}} = 0$ *and* $\zeta_{3,N}^{C_{pq}} = A_1$*, are the transversality conditions.*

In addition

$$\begin{aligned} u_i^{pqC_{rs}*} = \; & min\{max\{u^{min}, \\ & \frac{(\zeta_{1,i+1}^{C_{pq}} - \zeta_{2,i+1}^{C_{pq}})\beta_{rs} I_i^{C_{rs}*} S_i^{C_{pq}^*}}{A_{rs}}\}, u^{max}\}, \\ & i = 0,...,N-1 \end{aligned} \tag{3.9}$$

Proof. Using a discrete version of Pontryagin's Maximum Principle in [3],[4],[19], and setting $S^{C_{pq}} = S^{C_{pq}^*}$, $E^{C_{pq}} = E^{C_{pq}^*}$, $I^{C_{pq}} = I^{C_{pq}^*}$ and $u^{pqC_{rs}} = u^{pqC_{rs}*}$ we obtain the following adjoint equations

$$\begin{aligned} \triangle\zeta_{1,i}^{C_{pq}} &= -\frac{\partial\mathscr{H}}{\partial S_i^{C_{pq}}} \\ &= -\frac{\partial\mathscr{H}}{\partial S_i^{C_{pq}}} \\ &= -\Big[(1-d)\,\zeta_{1,i+1}^{C_{pq}} \\ &\quad + \left(\beta_{pq} I_i^{C_{pq}} + \sum_{C_{rs}\in V_{pq}} u_i^{pqC_{rs}} \beta_{rs} I_i^{C_{rs}}\right)\left(\zeta_{2,i+1}^{C_{pq}} - \zeta_{1,i+1}^{C_{pq}}\right) \end{aligned}$$

$$\begin{aligned}\triangle\zeta_{2,i}^{C_{pq}} &= -\frac{\partial\mathscr{H}}{\partial E_i^{C_{pq}}}\\ &= -\left[\gamma\left(\zeta_{3,i+1}^{C_{pq}}-\zeta_{2,i+1}^{C_{pq}}\right)+(1-d)\,\zeta_{2,i+1}^{C_{pq}}\right]\end{aligned}$$

$$\begin{aligned}\triangle\zeta_{3,i}^{C_{pq}} &= -\frac{\partial\mathscr{H}}{\partial I_i^{C_{pq}}}\\ &= -\left[A_1+\beta_{pq}S_i^{C_{pq}}\left(\zeta_{2,i+1}^{C_{pq}}-\zeta_{1,i+1}^{C_{pq}}\right)+\theta\left(\zeta_{1,i+1}^{C_{pq}}-\zeta_{3,i+1}^{C_{pq}}\right)+(1-\alpha-d)\,\zeta_{3,i+1}^{C_{pq}}\right]\end{aligned}$$

with $\zeta_{1,N}^{C_{pq}}=0, \zeta_{2,N}^{C_{pq}}=0$, and $\zeta_{3,N}^{C_{pq}}=A_1$ are the transversality conditions.

In order to obtain the optimality condition, we calculate the derivative of H with respect to $u_i^{pqC_{rs}}$, and we set it equal to zero

$$\frac{\partial\mathscr{H}}{\partial u_i^{pqC_{rs}}}=A_{rs}u_i^{pqC_{rs}}-\zeta_{1,i+1}^{C_{pq}}\beta_{rs}I_i^{C_{rs}}S_i^{C_{pq}}+\zeta_{2,i+1}^{C_{pq}}\beta_{rs}I_i^{C_{rs}}S_i^{C_{pq}}=0$$

Then, we obtain

$$u_i^{pqC_{rs}}=\frac{(\zeta_{1,i+1}^{C_{pq}}-\zeta_{2,i+1}^{Cpq})\beta_{rs}I_i^{C_{rs}}S_i^{C_{pq}}}{A_{rs}}$$

By the bounds in U_{pq}, we finally obtain the characterization of the optimal controls $u_i^{pqC_{rs}*}$ as

$$\begin{aligned}u_i^{pqC_{rs}*} &= min\{max\{u^{min},\\ &\quad\frac{(\zeta_{1,i+1}^{C_{pq}}-\zeta_{2,i+1}^{C_{pq}})\beta_{rs}I_i^{C_{rs}*}S_i^{C_{pq}*}}{A_{rs}}\},u^{max}\},\\ &\quad i=0,...,N-1,,C_{rs}\in V_{pq}\end{aligned}\tag{3.10}$$

□

4. **Numerical results and discussions**

4.1. **Brief presentation.** Here, we present some examples of numerical simulations in the case when the studied domain Ω represents the assembly of 100 regions or cells (cities, towns, ...), which means $M=10$ (i.e. a grid of 10×10 cells). We write and compile a code in MATLAB^M

$S_0^{C_{pq}}$	$E_0^{C_{pq}}$	$I_0^{C_{pq}}$	α	β	d	θ	γ
50	0	0	0.002	0.0003	0.0001	0.0002	0.002

TABLE 1. Parameters values of α, β, d, θ and γ associated to a cell C_{pq}, which are utilized for the resolution of all multi-regions discrete-time systems (3.1)-(3.2)-(3.3) and (3.6)-(3.7)-(3.8), and then leading to simulations obtained from Figure 1 to Figure 4, with the initial conditions $S_0^{C_{pq}}$, $E_0^{C_{pq}}$, and $I_0^{C_{pq}}$ associated to any cell C_{pq} of Ω.

using data cited in Table 1. Optimality systems are solved based on discrete progressive-regressive schemes. Explicitly, at instant i, the states $S_i^{C_{pq}}$, $E_i^{C_{pq}}$ and $I_i^{C_{pq}}$ with an initial guess, are obtained based on a progressive scheme in time, while their adjoint variables $\zeta_{l,i}^{C_{pq}}$, $l = 1,2,3$ are obtained based on a regressive scheme in time because of the transversality conditions. Then, we update the optimal controls values (3.9) using the values of state and costate variables obtained in previous steps.

At the initial instant $i = 0$, susceptible people are homogeneously distributed with 50 individuals in each cell except at the lower-right corner cell C_{1010}, where we introduce 10 infected individuals and 40 susceptible ones.

In figures presented below, the redder part of the color-bars, contains larger numbers of individuals while the bluer part contains the smaller numbers.

In the following, we discuss with more details, the cellular simulations obtained, in the case when there are yet no controls.

4.2. **Cellular simulations without controls.** Figures 1., 2. and 3. depict dynamics of the susceptible, exposed and infected populations in the case when there is yet no control strategy, followed for the prevention of the epidemic, and we note that in all these figures presented here, simulations give us an idea about the spread of the disease in the case when the epidemic starts in a cell C_{pq} with $p = 10, q = 10$ (located in the lower corner of Ω). It represents the case when

the vicinity set V_{pq} associated to the source cell of infection, contains 3 cells).

For instance, in Figure 1, if we suppose there are 40 susceptible people in cell C_{1010} located at the lower-right corner of Ω, and 50 in each other cell, we can see that at instant $i = 150$, the number $S^{C_{1010}}$ becomes less important and takes a value close/or equal to 30, while $S^{C_{pq}}$ in cells of V_{1010} take values close/or equal to 20, and as we move away from $V_{1010} = \{C_{109}, C_{910}, C_{99}\}$, $S^{C_{pq}}$ remains important. At instant $i = 300$, we can observe that in many cells, $S^{C_{pq}}$ becomes less important, taking values between 0 and 10 while in cells that are located in/and near V_{1010}, while other cells that are located far away from the source of infection, conserve their values in 50. At instant $i = 450$, $S^{C_{pq}}$ becomes zero in most cells that belong to V_{1010}, and as more we go forward in time, $S^{C_{pq}}$ converge to zero in all cells except few cells that are located at the opposite corners and borders.

Figure 2. illustrates the rapid propagation of the exposed population when we suppose there are 10 infected people in cell C_{1010}, and no infection in all other cells. From this figure, we observe that at instant $i = 150$, the number $E^{C_{1010}}$ increases to bigger values close/or equal to 30 in cells that belong to V_{1010}, and as we move away from V_{1010}, $E^{C_{pq}}$ remains less important. At instant $i = 300$, we can see that in most cells, $E^{C_{pq}}$ becomes more important, taking values between 30 and 35 in cells that are close to V_{1010} and have 8 neighbors, while in cells that are located in the 7th row and 7th column, it takes values between 20 and 25, and as we move further, the number is less important. From these numerical results, we can deduce that once the infection arrives to the center or to the cells with 8 cells in their vicinity sets, the infection becomes more important compared to the case of the previous instant. In fact, as we can observe at instant $i = 450$, $E^{C_{pq}}$ takes values close/or equal to 25 in the cell from where the epidemic has started, 30 in V_{1010} and 35 near to it, and as we move away towards the center and further regions, infection is important taking values between 15 and 25 infected individuals except the ones that are located in/and close to the 3 opposite borders and corners even at instant $i = 600$. Near the center of Ω, the number of infected people which has increased to 35 at the previous instant, has been reduced in the final instant, because once a cell becomes highly exposed to infection, it loses an

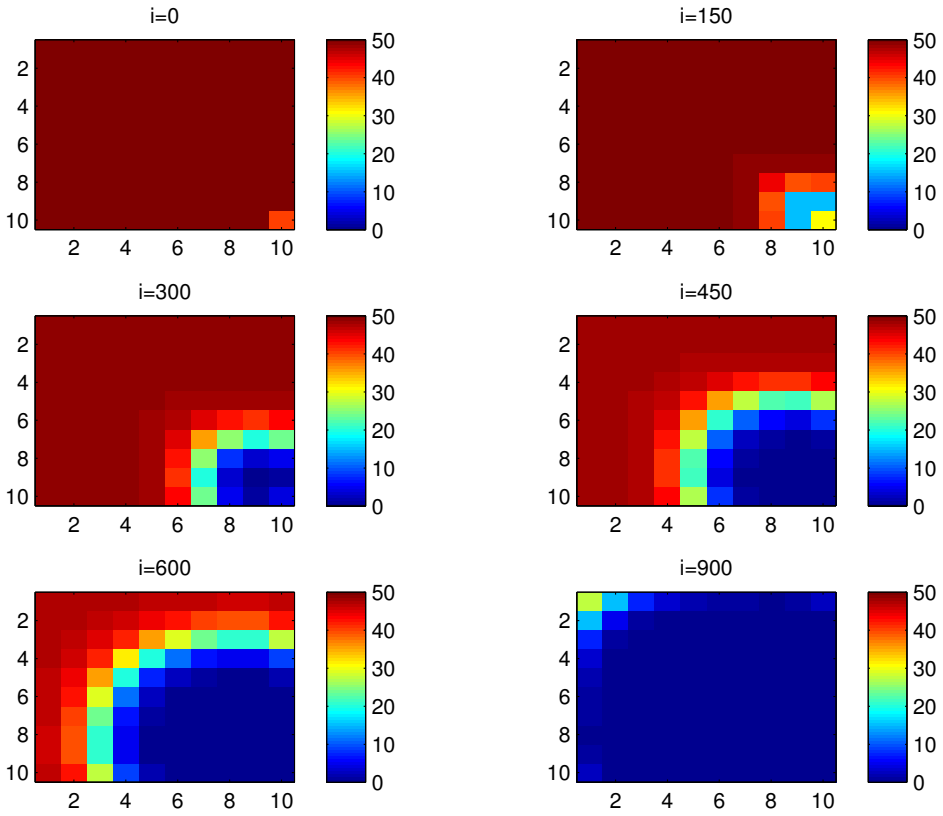

FIGURE 1. $S^{C_{pq}}$ behavior in the absence of controls.

important number of individuals which die or become infectious.

As we can also observe in Figure 3., at instant $i = 150$, $I^{C_{pq}}$ in cells of V_{1010}, is close/or equal to 5, and as we move away from V_{1010}, $I^{C_{pq}}$ is still zero. At instant $i = 300$, the number $I^{C_{pq}}$ in cells of V_{1010} is close/or equal to 12, except for distant cells where it remains zero. At instant $i = 450$, $I^{C_{pq}}$ takes values between 10 and 15 except at cells that are not very close to V_{1010} and at the opposite 3 corners and borders where there are yet no infected people. Finally, at further instants $I^{C_{pq}}$ converge to 20 in most cells at $i = 600$ and in all cells at $i = 900$ since as more we go forward in time, as more the infection gains other spaces. We can also observe at this final instant, that in cells which belong to V_{1010}, $I^{C_{pq}}$ becomes less important due to the effects of d, α and θ parameters.

4.3. **Cellular simulations with controls.** Figures 4., 5. and 6. depict dynamics of the SEIS populations when the travel-blocking vicinity optimal control strategy is followed.

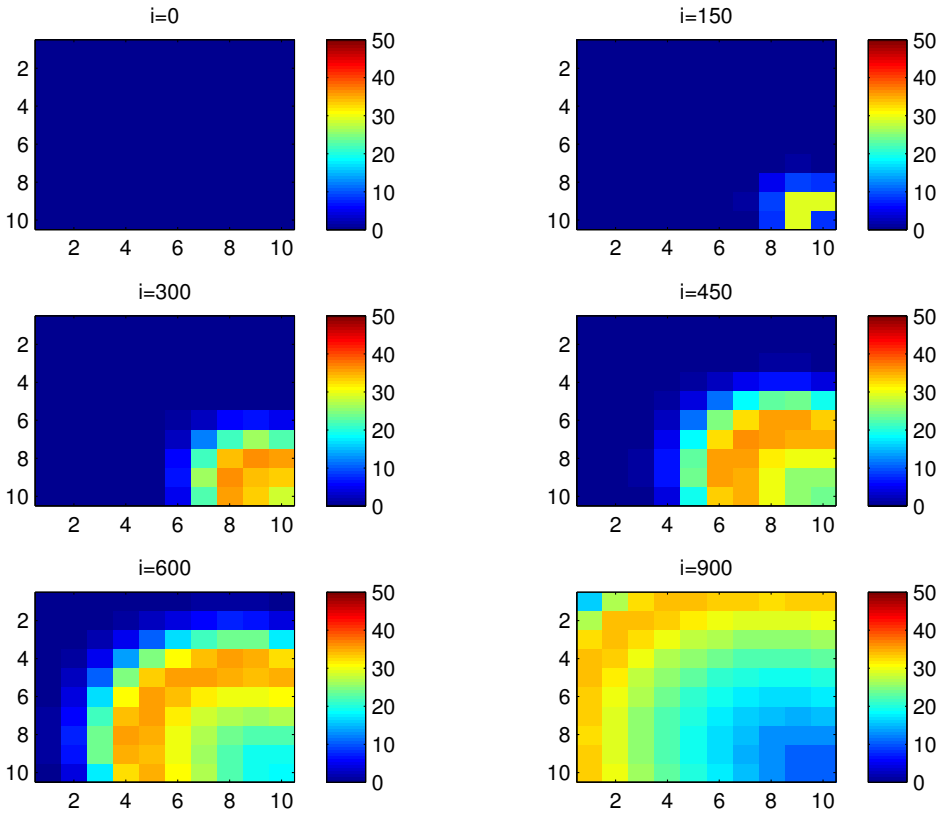

FIGURE 2. $E^{C_{pq}}$ behavior in the absence of controls.

In order to show the importance of the optimal control approach suggested in this paper, we consider C_{47} as example of a targeted cell which has 8 neighboring cells.

In Figure 4., as supposed also above, there are 40 susceptible people in cell C_{1010}, and 50 in each other cell. We can see that at instant $i = 150$, the numbers $S^{C_{1010}}$ and $S^{C_{pq}}$ are at most the same as in the case when there was no control strategy. At instant $i = 300$, we can observe that in most cells, $S^{C_{pq}}$ becomes less important, taking the value of 30 at the source of infection, 20 at V_{1010}, values between between 38 and 42 in cells that are close to V_{1010}, and as more we move away from V_{1010}, there is no change. The controlled cell C_{47} contains 45 susceptible people at instant $i = 450$, the number of susceptible people in the controlled cell conserved its value in 50, which is not also exactly the same as in the case when there was yet no control strategy since in Figure 2., $S^{C_{pq}}$ has decreased more significantly. Thus, we can deduce that

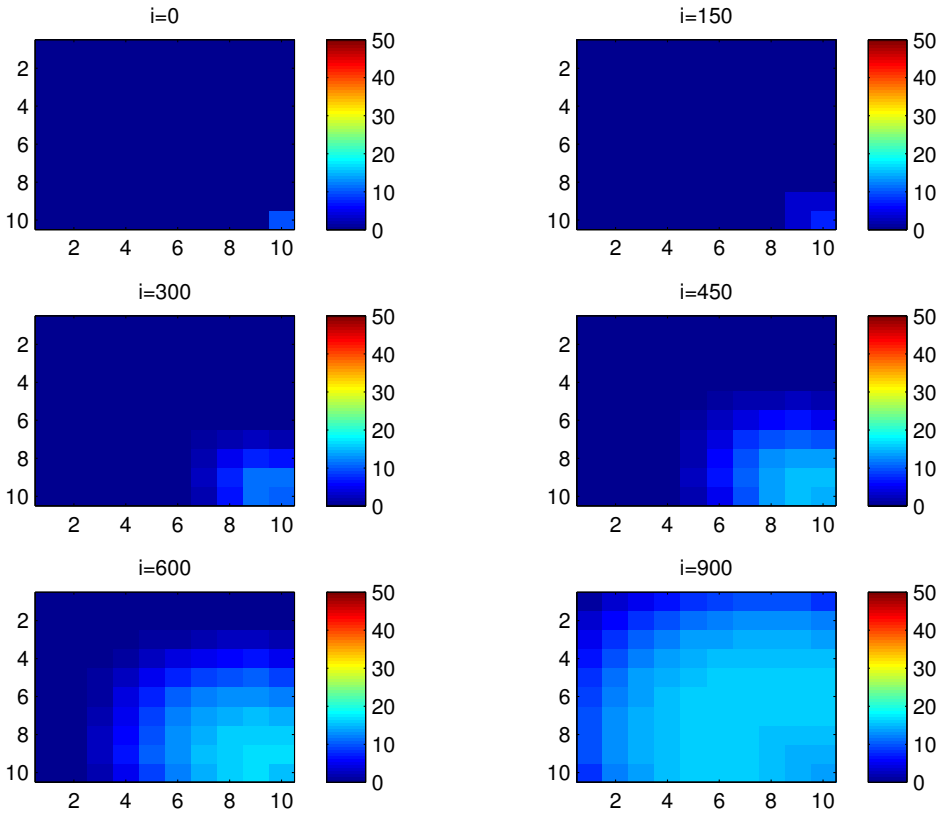

FIGURE 3. $I^{C_{pq}}$ behavior in the absence of controls.

the travel-blocking vicinity optimal control strategy has proved its effectiveness earlier in time. At instants $i = 600$ and $i = 900$, $S^{C_{pq}}$ is also the same as done before but fortunately again, we reach our goal in keeping the number $S^{C_{47}}$ close to its initial value despite some small decrease. Thus, this demonstrates that most of movements of infected people coming from the vicinity set $V^{C_{47}}$, have been restricted in final times.

In Figure 5., we can deduce that at instant $i = 150$, the numbers $E^{C_{1010}}$ and $E^{C_{pq}}$ are at most the same, as shown in the absence of controls. At instant $i = 300$, we can see that in most cells, $E^{C_{pq}}$ is also similar to the case in Figure 2. At instant $i = 450$, $E^{C_{pq}}$ does not increase in cell C_{47} as in Figure 2. while other cells are always exposed to infection. At instant $i = 600$, most cells C_{pq} begin to lose some of their exposed individuals due to death or because they become infectious, while at the same and final instants, $E^{C_{47}}$ does not exceed 2 or less exposed individuals.

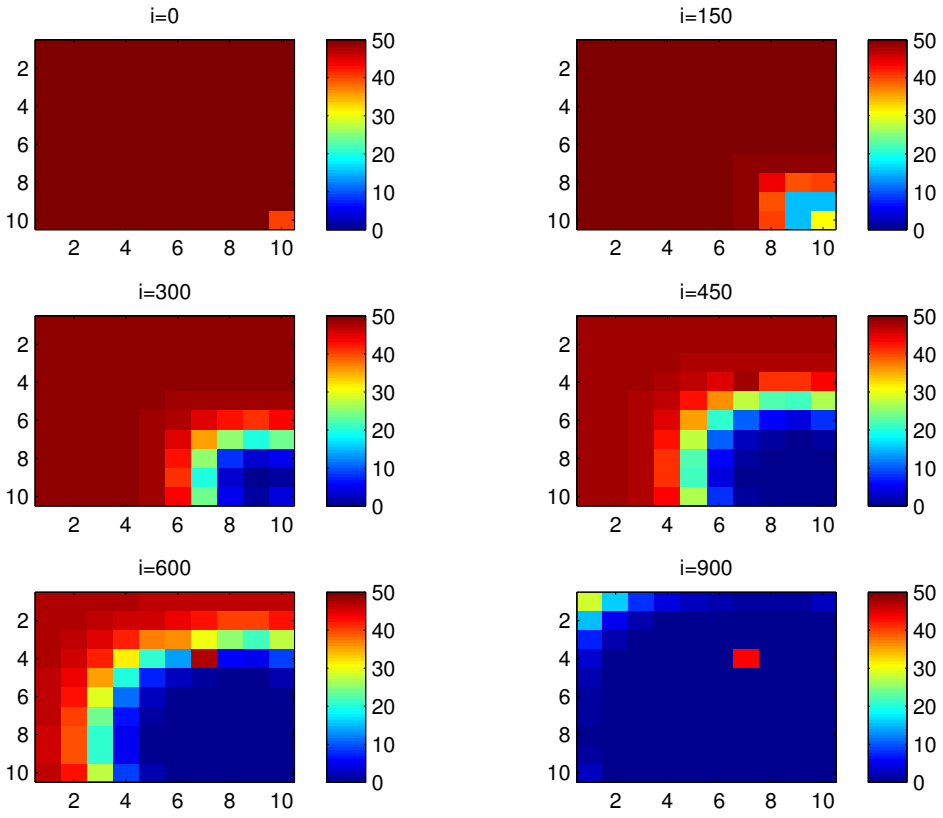

FIGURE 4. $S^{C_{pq}}$ behavior in the presence of optimal controls (3.9).

In Figure 6., no change in the number of infected people can be observed at instants $i = 150, 300$ and $i = 450$. However, at further times, we can observe from instant $i = 600$ that $I^{C_{47}}$ conserves its value in zero, which proves the effectiveness of the followed control strategy.

5. Conclusion

We devised a multi-regions SEIS discrete-time model which describes infection dynamics related to the spread of an epidemic in different regions via travel. Regions have been assembled in one grid of cells, in order to exhibit the impact of infection which comes from the vicinity of a cell. In fact, by this kind of representations, we have succeeded to show the effectiveness of the travel-blocking vicinity optimal control approach when it is applied to the example of only one cell, an then, we demonstrated that when we restrict movements of infected people coming from the vicinity of one targeted cell, we can keep this cell safe, and without/or with no important infection.

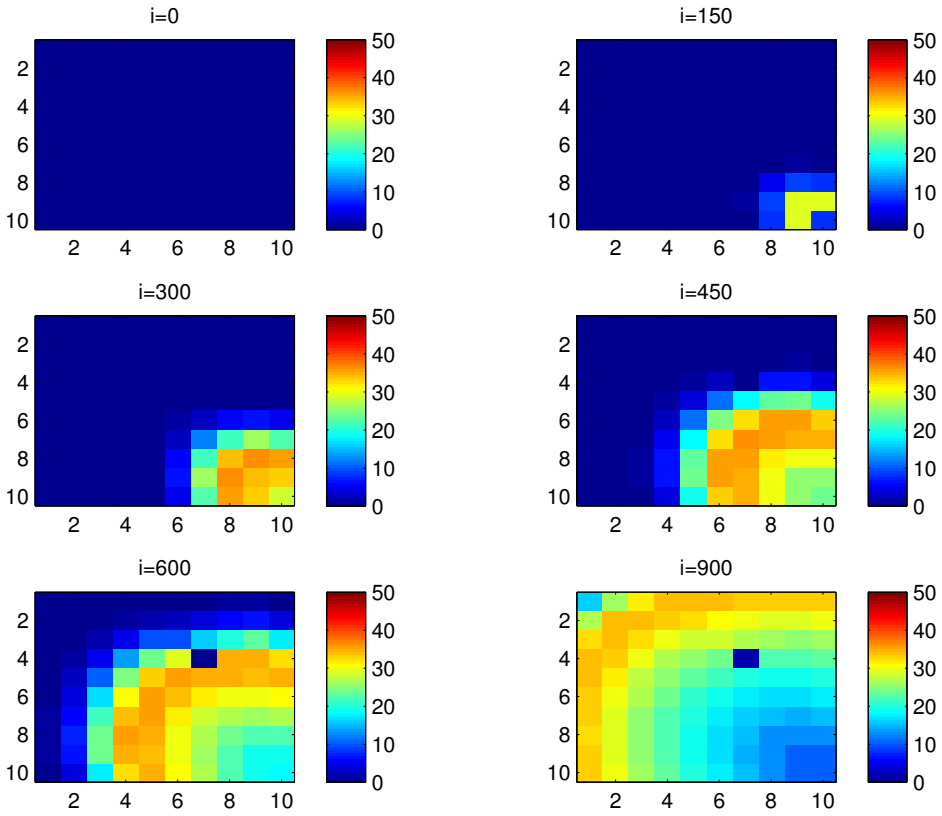

FIGURE 5. $E^{C_{pq}}$ behavior in the presence of optimal controls (3.9).

Conflict of Interests

The authors declare that there is no conflict of interests.

Acknowledgement

This work is supported by the Systems Theory Network (Réseau Théorie des Systèmes), and Hassan II Academy of Sciences and Technologies-Morocco.

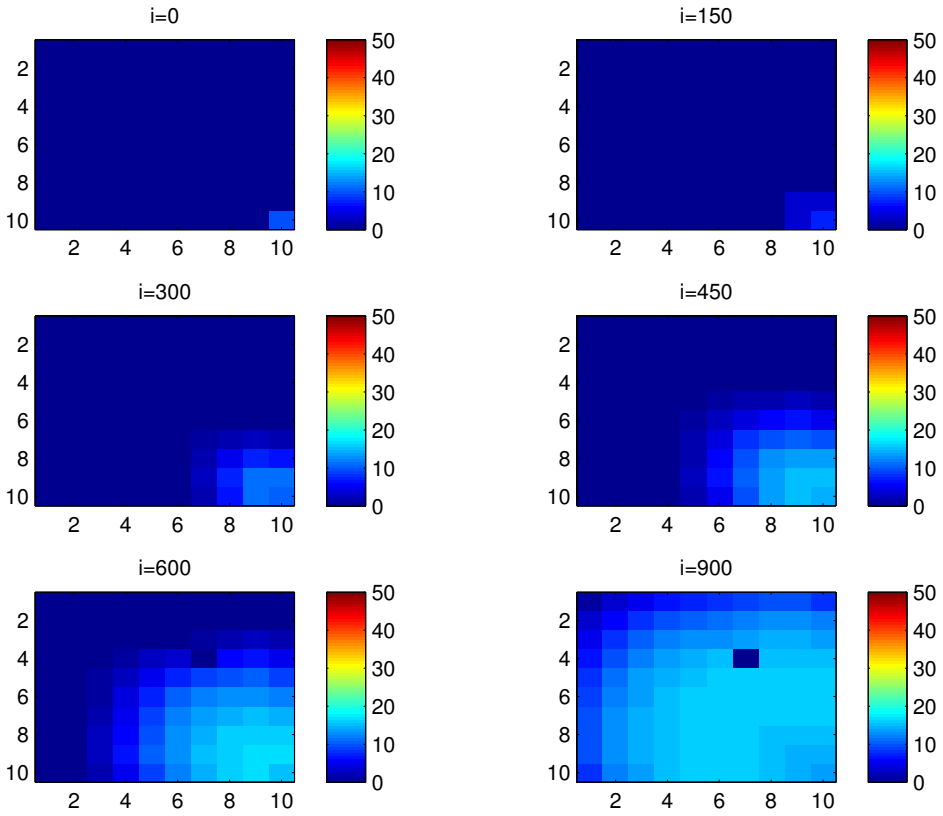

FIGURE 6. $I^{C_{pq}}$ behavior in the presence of optimal controls (3.9).

REFERENCES

[1] López, M., Peinado, A., & Ortiz, A., A SEIS Model for Propagation of Random Jamming Attacks in Wireless Sensor Networks; In International Conference on EUropean Transnational Education (pp. 668-677). Springer International Publishing. (2016, October). (2016).

[2] Xu, R., Zhang, S., & Zhang, F., Global dynamics of a delayed SEIS infectious disease model with logistic growth and saturation incidence; Math. Methods Appl. Sci. 39 (12) (2016), 3294–3308.

[3] Zakary, O., Rachik, M., Elmouki, I., On the analysis of a multi-regions discrete SIR epidemic model: an optimal control approach; I. Int. J. Dynam. Control (2016) 1-14, doi:10.1007/s40435-016-0233-2.

[4] Zakary, O., Rachik, M., Elmouki, I., A new analysis of infection dynamics: multi-regions discrete epidemic model with an extended optimal control approach; I. Int. J. Dynam. Control (2016), 1-10, doi:10.1007/s40435-016-0264-8.

[5] Zakary, O., Larrache, A., Rachik, M., Elmouki, I., Effect of awareness programs and travel-blocking operations in the control of HIV/AIDS outbreaks: a multi-domains SIR model; Adv. Differ. Equ. 1 (2016), 1-17.

[6] Zakary, O., Rachik, M., Elmouki, I., A multi-regional epidemic model for controlling the spread of Ebola: awareness, treatment, and travel-blocking optimal control approaches; Math. Methods Appl. Sci. 40 (4) (2017), 1265–1279.

[7] Abouelkheir, I., El Kihal, F., Rachik, M., Zakary, O., Elmouki, I. A Multi-Regions SIRS Discrete Epidemic Model With a Travel-Blocking Vicinity Optimal Control Approach on Cells. Br. J. Math. Comput. Sci. 20(4)(2017). 1-16.

[8] El Kihal, F., Rachik, M., Zakary, O., Elmouki, I. A multi-regions SEIRS discrete epidemic model with a travel-blocking vicinity optimal control approach on cells. Int. J. Adv. Appl. Math. Mech. 4(3)(2017). 60-71.

[9] Sánchez-Vizcaíno, J. M., Mur, L., & Martínez-López, B., African swine fever: an epidemiological update; Transboundary and Emerging Diseases, 59 (2012), 27-35.

[10] Fray, M. D., Paton, D. J., & Alenius, S., The effects of bovine viral diarrhoea virus on cattle reproduction in relation to disease control; Animal Reproduction Science, 60 (2000), 615-627.

[11] Thiaucourt, F., Yaya, A., Wesonga, H., Huebschle, O. J. B., Tulasne, J. J., & Provost, A., Contagious bovine pleuropneumonia: a reassessment of the efficacy of vaccines used in Africa; Ann. N. Y. Acad. Sci. 916 (1) (2000), 71-80. .

[12] Grubman, M. J., & Baxt, B., Foot-and-mouth disease; Clinical Microbiol. Rev. 17 (2) (2004), 465-493.

[13] Afia, N., Manmohan Singh, and David Lucy, Numerical study of SARS epidemic model with the inclusion of diffusion in the system; Appl. Math. Comput. 229 (2014), 480-498.

[14] Zakary, O., Rachik, M., Elmouki, I., On the impact of awareness programs in HIV/AIDS prevention: an SIR model with optimal control; Int. J. Comput. Appl, 133 (9) (2016), 1-6.

[15] Samanta, G.P., Permanence and extinction of a nonautonomous HIV/AIDS epidemic model with distributed time delay; Nonlinear Anal., Real World Appl. 12 (2) (2011), 1163-1177.

[16] Chunxiao, D., Tao, N., Zhu, Y., A mathematical model of Zika virus and its optimal control; In Control Conference (CCC), 2016 35th Chinese, pp. 2642-2645. TCCT, (2016).

[17] Wandi, D., Hendon, R., Cathey, B., Lancaster, E., and Germick. R., Discrete time optimal control applied to pest control problems; Involve, 7 (4) (2014), 479-489.

[18] Dabbs, K., Optimal control in discrete pest control models; Thesis. trace.tennessee.edu. (2010).

[19] Sethi S.P., Thompson, G.L., What is optimal control theory?; Springer, US, pp 1-22. (2000).